ACADEMIC PRESS

Available online at www.sciencedirect.com

SCIENCE DIRECT

Journal of Sound and Vibration 270 (2004) 639–655

JOURNAL OF SOUND AND VIBRATION

www.elsevier.com/locate/jsvi

Preconditioning multichannel adaptive filtering algorithms using EVD- and SVD-based signal prewhitening and system decoupling

M.R. Bai[a,]*, S.J. Elliott[b]

[a] *Department of Mechanical Engineering, National Chiao-Tung University, 1001 Ta-Hsueh Road, Hsin-Chu 300, Taiwan, ROC*

[b] *SPCG, Institute of Sound and Vibration Research, University of Southampton, Highfield, Southampton SO17 1BJ, UK*

Received 29 July 2002; accepted 5 February 2003

Abstract

It is well known that the convergence rate of multichannel LMS-based algorithms is limited by the correlation properties of the reference signals and the cross-coupling within the plant dynamics. These factors give rise to excessive eigenvalue spread and slow convergence rate of a gradient descent algorithm. A preconditioning technique is developed in this study for the multichannel LMS algorithm so as to improve its convergence rate. Signal prewhitening and system decoupling are the two key elements of the proposed techniques. Preconditioning filters are first formulated in the frequency domain by using eigenvalue decomposition and singular value decomposition. These filters are then transformed into the time domain with causality taken into account. The preconditioning filters are incorporated into a multichannel LMS algorithm, where the reference signals are prewhitened and the plants are decoupled prior to the adaptation process. Simulations for a two-channel/one listener cross-talk cancellation problem illustrate the effectiveness of the preconditioning technique in improving the convergence rate of the adaptive algorithms.

1. Introduction

The least-mean-square (LMS) algorithm has become a widely used adaptive filtering method, owing to its simplicity and adaptability to non-stationarity in the signals being processed. The

*Corresponding author. Fax: +886-3-5720634.

E-mail addresses: msbai@mail.nctu.edu.tw (M.R. Bai), sje@isvr.soton.ac.uk (S.J. Elliott).

0022-460X/03/$ - see front matter
doi:10.1016/S0022-460X(03)00150-0

LMS algorithm and its variants have found application in many areas. Among which, active noise and vibration control (ANVC) [1–4], and cross-talk cancellation system (CCS) of audio signals [5,6] are two useful applications of the LMS algorithm. In ANVC, one seeks to suppress undesired disturbance using "counter" sound or vibration, whereas in CCS one aims to cancel the cross-coupling paths between the reproducing loudspeakers and the ears of a listener. Both problems boil down to "inverse filtering" of generally non-invertible plants (with delays and/or non-minimum phase zeros). The LMS algorithm is just the simple approach well suited to approximating inverse plants.

Despite the simplicity, LMS suffers from the problems of slow convergence, which, in the multichannel context, may be due to two distinct effects. First, the reference signals are not white and may also be cross-correlated. Second, the multiple-input–multiple-output (MIMO) response of the system under control, which will be referred to as the plant, may have non-flat dynamics and cross-coupling paths. These factors give rise to excessive eigenvalue spread and thus slow convergence rate of gradient descent algorithms. To cope with this problem, methods have been reported in literature, particularly for signal prewhitening. Cook and Elliott investigated the connection between the prediction error filter and spectral factorization [7]. Douglas et al. developed two prewhitening techniques within gradient update to improve the convergence of stochastic gradient adaptive filters [8]. Proudler et al. suggested a preconditioning filter, which reduces eigenvalue spread of the input signal to increase the convergence speed of the LMS algorithm [9].

Motivated by the structure of the optimal Wiener filters for stochastic signals, a recent paper has suggested a modified LMS algorithm to overcome many of the slow convergence problems, by separately preconditioning the reference and plant dynamics. Two crucial steps required by this method are the computation of spectral factorization of the reference signals and minimum-phase/all-pass decomposition of the secondary plants [10]. In practical application of this method, a natural question is how to actually compute these factorizations. In the scalar case, this is in principle straightforward: compute the poles and zeros and replace the unstable ones with their conjugate reciprocals. Unfortunately, generalizing this method to the matrix case is not trivial. Some methods have been reported in literature for computing the matrix-valued spectral factorization. An excellent review of these methods can be found in the book by Kailath et al. [11]. However, a common problem associated with these factorization methods is that they generally rely on accurate modelling of the MIMO systems in terms of state-space form, which is extremely difficult for high order systems frequently encountered in sound and vibration problems.

To alleviate the problems associated with explicit modelling of high order multichannel systems, as required in the previous method, this paper proposes an alternative approach for computing the preconditioning filters, based on only power spectral density functions of the reference signals and the frequency response functions of secondary plants both of which can be readily measured by experimental means. Similar to the spectral factorization and minimum-phase/all-pass decomposition in Ref. [10], signal prewhitening and system decoupling play two key roles in the proposed technique. These methods are numerically straightforward and do not rely on any explicit modelling nor identification of systems, which is indeed a desirable feature from the application point of view. Although these methods are only intended in this paper for improving the convergence of LMS adaptive algorithms, they are fundamentally important to many other areas of signal processing and control engineering as well, e.g., cross-talk cancellation in audio signal processing, channel equalization in communication, image processing in geophysical exploration, inverse modelling and plant decoupling in decentralized control, etc. [3,12,13].

In the method proposed in this paper, preconditioning filters are first formulated in the frequency domain by using eigenvalue decomposition (EVD) and singular value decomposition (SVD). The filters are then converted to impulse responses in the time domain, or FIR filter coefficients, with causality taken into account. Finally, the preconditioning filters are incorporated into the multichannel LMS algorithm, where the reference signals are prewhitened and the secondary plants are decoupled prior to the adaptation process. Numerical simulation was carried out to investigate the performance of the preconditioned multichannel LMS algorithm. Results will be presented and discussed in terms of convergence properties of the algorithms.

2. Preconditioning techniques

In this section, the preconditioning filters will first be formulated in the frequency domain. Then, the frequency response functions of the precondition filter will be converted in the time domain into causal FIR filters. Finally, the preconditioning filters will be introduced to precondition the multichannel LMS algorithm.

2.1. The frequency-domain formulation of the preconditioning filters

As mentioned previously, the LMS algorithm may suffer from problems with slow convergence due to two effects: the reference signals are not white and may also be cross-correlated, and the plant may have non-flat dynamics and cross-coupling paths. It is then highly desirable to precondition the signals and the systems such that the overall convergence property of the adaptation process is altered. In particular, EVD is exploited for prewhitening and decorrelating the reference signals, whereas SVD is exploited for equalizing and decoupling the secondary plants.

First, the prewhitening filters for reference signals will be addressed. Assume that K discrete-time real-valued random reference signals are stationary, but possibly correlated, and are described by the vector

$$\mathbf{x}(n) = [x_1(n) \ldots x_K(n)]^{\mathrm{T}}, \tag{1}$$

where the superscript "T" denotes matrix transpose. The correlation matrix of signal $\mathbf{x}(n)$ can be defined as

$$\mathbf{R_{xx}}(m) = E\{\mathbf{x}(n+m)\mathbf{x}^{\mathrm{H}}(n)\}, \quad -\infty < m < \infty, \tag{2}$$

where the superscript "H" denotes the Hermitian transpose. Note that

$$\mathbf{R_{xx}}(m) = \mathbf{R}^{\mathrm{H}}_{\mathbf{xx}}(-m), \quad -\infty < m < \infty. \tag{3}$$

The power spectral density matrix is defined by taking the discrete-time Fourier transform of the correlation matrix

$$\mathbf{S_{xx}}(\mathrm{e}^{\mathrm{j}\omega}) = \sum_{m=-\infty}^{\infty} \mathbf{R_{xx}}(m)\mathrm{e}^{-\mathrm{j}\omega m}, \quad \mathrm{j} = \sqrt{-1}. \tag{4}$$

For stable sequences, the above definition converges for all $\omega \in [0, 2\pi]$ and has the following properties:

(i) Hermitian symmetry:

$$\mathbf{S_{xx}}(e^{j\omega}) = \mathbf{S}^{H}_{\mathbf{xx}}(e^{j\omega}). \tag{5}$$

(ii) Non-negativity:

$$\mathbf{S_{xx}}(e^{j\omega}) \geq 0, \quad -\pi \leq \omega \leq \pi. \tag{6}$$

These two properties lead immediately to the fact that the $K \times K$ power spectral density matrix $\mathbf{S_{xx}}(e^{j\omega})$ is a positive semi-definite Hermitian matrix. For any such matrix, an EVD always exists [14]

$$\mathbf{S_{xx}}(e^{j\omega}) = \mathbf{Q}(e^{j\omega})\mathbf{D}(e^{j\omega})\mathbf{Q}^{H}(e^{j\omega}), \tag{7}$$

where $\mathbf{D}(e^{j\omega})$ is a diagonal matrix consisting of the non-negative eigenvalues of $\mathbf{S_{xx}}(e^{j\omega})$, and $\mathbf{Q}(e^{j\omega})$ is a unitary matrix consisting of normalized eigenvectors. Now, let

$$\mathbf{w}(e^{j\omega}) = \mathbf{F}_{w}(e^{j\omega})\mathbf{x}(e^{j\omega}), \tag{8}$$

where the "preconditioning filter" is defined as

$$\mathbf{F}_{w}(e^{j\omega}) = \mathbf{D}^{-1/2}(e^{j\omega})\mathbf{Q}^{H}(e^{j\omega}). \tag{9}$$

The matrix $\mathbf{D}^{-1/2}(e^{j\omega})$ exists whenever the reference signals are "spectrally rich" within the control bandwidth. The term, spectrally rich, refers to the signals having non-zero frequency contents throughout the band of interest, e.g., a broadband noise, such that the inverse of the matrix $\mathbf{D}(e^{j\omega})$ exists.

Using the identity of matrix-valued linear time-invariant systems [11],

$$\mathbf{S_{ww}}(e^{j\omega}) = \mathbf{F}_{w}(e^{j\omega})\mathbf{S_{xx}}(e^{j\omega})\mathbf{F}^{H}_{w}(e^{j\omega}) \tag{10}$$

we can then diagonalize the power spectral density matrix of the filtered signal, $\mathbf{w}$, into an identity matrix

$$\mathbf{S_{ww}}(e^{j\omega}) = \mathbf{D}^{-1/2}(e^{j\omega})\mathbf{Q}^{H}(e^{j\omega})\mathbf{Q}(e^{j\omega})\mathbf{D}(e^{j\omega})\mathbf{Q}^{H}(e^{j\omega})\mathbf{Q}(e^{j\omega})(\mathbf{D}^{-1/2}(e^{j\omega}))^{H} = \mathbf{I}, \tag{11}$$

where the property of the unitary matrix, $\mathbf{Q}^{H}(e^{j\omega})\mathbf{Q}(e^{j\omega}) = \mathbf{Q}(e^{j\omega})\mathbf{Q}^{H}(e^{j\omega}) = \mathbf{I}$, has been invoked. It follows that the signal, $\mathbf{x}$, has been "prewhitened" and "decorrelated" by means of the filtering $\mathbf{F}_{w}(e^{j\omega})$. The overall idea is schematically shown in the block diagram of Fig. 1.

By the same token, a system can be "diagonalized" by orthogonal transformations. A more universal decomposition, SVD, is exploited in this case because a system matrix is in general not

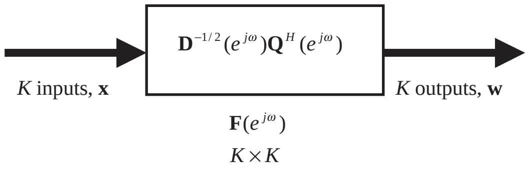

Fig. 1. The frequency-domain formulation of the signal prewhitening and decorrelating filter.

Hermitian, and even not square. Assume that a stable MIMO linear time-invariant system with M inputs and L outputs is described by the $L \times M$ frequency response matrix $\mathbf{G}(e^{j\omega})$. The following factorization, the SVD, of $\mathbf{G}(e^{j\omega})$ is always possible [14]

$$\mathbf{G}(e^{j\omega}) = \mathbf{U}(e^{j\omega})\mathbf{\Sigma}(e^{j\omega})\mathbf{V}^{H}(e^{j\omega}), \quad (12)$$

where $\mathbf{U}(e^{j\omega})$ and $\mathbf{V}(e^{j\omega})$ are an $L \times L$ unitary matrix and an $M \times M$ unitary matrix, respectively, and $\mathbf{\Sigma}(e^{j\omega})$ is an $L \times M$ matrix whose entries are all zero except for the non-negative diagonal elements called singular values. The number of non-zero (positive) singular values determines the rank of the matrix $\mathbf{G}(e^{j\omega})$. Now, let

$$\mathbf{G}_{mi}(e^{j\omega}) = \mathbf{V}(e^{j\omega})\mathbf{\Sigma}^{+}(e^{j\omega}) \quad (13)$$

and

$$\mathbf{G}_{ai}(e^{j\omega}) = \mathbf{U}^{H}(e^{j\omega}), \quad (14)$$

where the superscript "+" denotes the *pseudo-inverse* operation with exceedingly small singular values in the matrix $\mathbf{\Sigma}$ replaced by zeros or small constant values. This is a "regularization" technique in matrix inversion commonly used in conjunction with the application of the SVD algorithm. Note also that

$$\mathbf{G}_{ai}(e^{j\omega})\mathbf{G}_{ai}^{H}(e^{j\omega}) = \mathbf{U}^{H}(e^{j\omega})\mathbf{U}(e^{j\omega}) = \mathbf{I} \quad (15)$$

and

$$\mathbf{G}_{mi}(e^{j\omega})\mathbf{G}_{mi}^{H}(e^{j\omega}) = (\mathbf{G}^{H}(e^{j\omega})\mathbf{G}(e^{j\omega}))^{+}. \quad (16)$$

The notion of preconditioning can be realized by noting that

$$\mathbf{G}(e^{j\omega})\mathbf{G}_{mi}(e^{j\omega}) = \mathbf{U}(e^{j\omega})\mathbf{\Sigma}(e^{j\omega})\mathbf{V}^{H}(e^{j\omega})\mathbf{V}(e^{j\omega})\mathbf{\Sigma}^{+}(e^{j\omega}) = \hat{\mathbf{U}}(e^{j\omega})$$

which amounts to the "equalization" since $\hat{\mathbf{U}}(e^{j\omega})$ is "almost" unitary in that it is the truncated version of $\mathbf{U}(e^{j\omega})$, retaining only the orthonormal basis of the range space of $\mathbf{G}(e^{j\omega})$, and the remaining $(L-M)$ columns are replaced with zero vectors. A unitary matrix is all-pass in nature and is thus energy preserving. When $\mathbf{G}(e^{j\omega})$ is non-singular, the equalization process becomes exact. On the other hand,

$$\mathbf{G}_{ai}(e^{j\omega})\mathbf{G}(e^{j\omega})\mathbf{G}_{mi}(e^{j\omega}) = \mathbf{U}^{H}(e^{j\omega})\hat{\mathbf{U}}(e^{j\omega}) = \hat{\mathbf{I}} \quad (17)$$

which amounts to "diagonalizing" or "decoupling" of the system $\mathbf{G}(e^{j\omega})$, since $\hat{\mathbf{I}}$ is a truncated identity matrix, with the rank-deficient $(L-M)$ diagonal elements replaced with zeros. Likewise, when $\mathbf{G}(e^{j\omega})$ is non-singular, the diagonalization process becomes exact. In this setting, the system, $\mathbf{G}(e^{j\omega})$, has been "equalized" and "decoupled" via prefiltering $\mathbf{G}_{mi}(e^{j\omega})$ and postfiltering $\mathbf{G}_{ai}(e^{j\omega})$. The overall idea is schematically shown in the block diagram of Fig. 2.

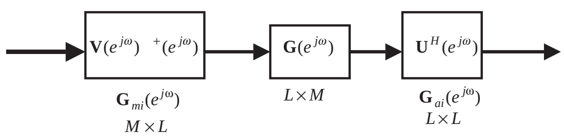

Fig. 2. The frequency-domain formulation of the plant equalization and decoupling filter.

It is remarked that the notations used above were deliberately chosen as the reminiscent of Ref. [10]. One can readily identify the correspondence between the spectral factorization and minimum-phase/all-pass decomposition in Ref. [10], and EVD and SVD in this paper. In comparison with some existing methods [11] which are algebraically cumbersome and could present numerical difficulties, the EVD- and SVD-based methods presented in this paper are numerically stable and do not rely on any explicit modelling nor identification of system, which is indeed a desirable feature from the application point of view. Although these methods are only intended in this paper for improving the convergence of the LMS adaptive algorithms, they are important in their own right for many signal processing and control applications.

2.2. Time-domain formulation of the preconditioning filters

The above-mentioned preconditioning filters were formulated in the frequency domain, where stability of systems has been assumed. Impulse response matrices of the filters can be obtained by taking inverse discrete-time Fourier transform (or FFT in practice) of the frequency response matrices. In implementation, appropriate delay and truncation must be introduced to ensure the causality of the filters. These procedures apply to both prewhitening of reference signals and the decoupling of plants. The complete procedures are summarized as follows:

(i) Calculate the frequency response matrix of $\mathbf{F}_w(e^{j\omega})$, $\mathbf{G}_{mi}(e^{j\omega})$, or $\mathbf{G}_{ai}(e^{j\omega})$, according to the method mentioned above. For example, a 2×2 frequency response matrix should take the form

$$\mathbf{H}(e^{j\omega}) = \begin{bmatrix} H_{11}(e^{j\omega}) & H_{21}(e^{j\omega}) \\ H_{12}(e^{j\omega}) & H_{22}(e^{j\omega}) \end{bmatrix}. \tag{18}$$

(ii) Obtain the impulse response matrix by taking the inverse FFT of the frequency response matrix

$$\mathbf{h}(n) = \begin{bmatrix} h_{11}(n) & h_{21}(n) \\ h_{12}(n) & h_{22}(n) \end{bmatrix} \tag{19}$$

with reference to the symmetry property of the frequency response matrices,

$$\mathbf{H}(e^{-j\omega}) = \mathbf{H}^*(e^{j\omega}). \tag{20}$$

(iii) Delay $\mathbf{h}(n)$ to form a new impulse response matrix

$$\hat{\mathbf{h}}(n) = \begin{bmatrix} \hat{h}_{11}(n) & \hat{h}_{21}(n) \\ \hat{h}_{12}(n) & \hat{h}_{22}(n) \end{bmatrix}. \tag{21}$$

It is stressed here that sufficient number of sample delays must be included to ensure the causality of all entries of the impulse response matrix. This will in effect introduce a linear phase shift to the filter. Record the number of sample delay as J.

(iv) Truncate the non-causal part of $\hat{\mathbf{h}}(n)$ appropriately to obtain the coefficients of FIR filters

$$\hat{\mathbf{H}}(z) = \begin{bmatrix} \hat{H}_{11}(z) & \hat{H}_{21}(z) \\ \hat{H}_{12}(z) & \hat{H}_{22}(z) \end{bmatrix}. \tag{22}$$

2.3. Preconditioning the multichannel LMS algorithms

One of the remarkable applications of the aforementioned signal prewhitening and system decoupling techniques is its application to improve convergence of adaptive algorithms. Before embarking on the discussion of our method, a brief review of the multichannel preconditioned LMS algorithm originally presented in Ref. [10] is given.

As noted by many researchers, the multichannel LMS algorithms may suffer from the problem of slow convergence due to [2]

(i) the auto-correlation properties of each of the random reference signals;
(ii) the cross-correlation between the individual reference signals;
(iii) the dynamic response of each path in the plant response;
(iv) the cross-coupling between the individual paths in the multichannel plant response.

A method for preconditioning the reference signals and plants was proposed in Ref. [10], using spectral factorization and minimum-phase/all-pass decomposition, respectively. Consider the general multichannel feedforward control problem depicted in Fig. 3, where $\mathbf{x}(n)$, $\mathbf{u}(n)$, $\mathbf{e}(n)$, and $\mathbf{d}(n)$ represent K reference signals, M control signals, L error signals, and L disturbance signals. $\mathbf{W}(z)$ and $\mathbf{G}(z)$ are an $M \times K$ matrix and an $L \times M$ matrix of the feedforward controller and the secondary plant, respectively. The method in Ref. [10] was motivated by the following Wiener–Hoff solution of the problem in Fig. 3.

$$\mathbf{W}_{opt}(z) = -\mathbf{G}_{min}^{-1}(z)\{\mathbf{G}_{all}^{\mathrm{T}}(z^{-1})\mathbf{S}_{xd}(z)\mathbf{F}^{-\mathrm{T}}(z^{-1})\}_{+}\mathbf{F}^{-1}(z), \tag{23}$$

where $\mathbf{S}_{xd}(z)$ is the cross-spectral density matrix between the reference signal $\mathbf{x}(n)$ and the disturbance signal $\mathbf{d}(n)$, $\mathbf{F}(z)$ is the *spectral factorization* of the power spectral density matrix $\mathbf{x}(n)$, i.e.,

$$\mathbf{S}_{xx}(z) = \mathbf{F}(z)\mathbf{F}^{\mathrm{T}}(z^{-1}), \tag{24}$$

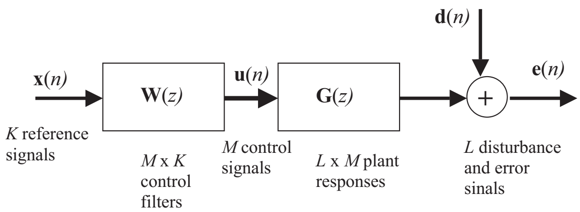

Fig. 3. Multichannel feedforward control problem.

where $\mathbf{G}_{min}(z)$ and $\mathbf{G}_{all}(z)$ denote the *minimum-phase* part and the *all-pass* part in the decomposition of $\mathbf{G}(z)$, i.e.,

$$\mathbf{G}(z) = \mathbf{G}_{all}(z)\mathbf{G}_{min}(z) \tag{25}$$

and "$\{\ \}_+$" denotes the z-transform of the causal part [15]. Rather than adapting the control filter matrix $\mathbf{W}(z)$ directly, using an ordinary multichannel LMS algorithm, the optimal solution in Eq. (23) suggests an alternative control architecture, as depicted in Fig. 4, where the controller is updated according to the rule

$$\mathbf{C}_i(n+1) = \mathbf{C}_i(n) - \alpha\mathbf{a}(n)\mathbf{v}^{\mathrm{T}}(n-i), \tag{26}$$

where α is the convergence coefficient and

$$\mathbf{a}(n) = \mathbf{G}_{all}^{\mathrm{T}}(z^{-1})\mathbf{e}(n), \tag{27}$$

$$\mathbf{v}(n) = \mathbf{F}^{-1}(z)\mathbf{x}(n). \tag{28}$$

The success of forgoing algorithm relies upon two key factorizations: the spectral factorization and the minimum-phase/all-pass decomposition. To the author's knowledge, no simple and reliable methods are available hitherto for reliable computation of these factorizations in multichannel cases.

In this paper, an alternative approach that bypasses the numerical difficulties encountered in the model-based factorizations is developed for preconditioning the multichannel adaptive algorithms. Without resorting to any spectral factorization, we prewhiten and decorrelate the reference signals by using the EVD in Section 2.1. Without resorting to any minimum-phase/all-pass decomposition, we equalize and decouple the secondary plants by using the SVD in Section 2.1. Causal and implementable FIR filters are then obtained using the delay and truncation method in Section 2.2, as symbolically expressed as

$$\mathbf{F}_w(\mathrm{e}^{\mathrm{j}\omega}) = \mathbf{D}^{-1/2}(\mathrm{e}^{\mathrm{j}\omega})\mathbf{Q}^{\mathrm{H}}(\mathrm{e}^{\mathrm{j}\omega}) \sim \hat{\mathbf{F}}_w(z), \tag{29}$$

$$\mathbf{G}_{mi}(\mathrm{e}^{\mathrm{j}\omega}) = \mathbf{V}(\mathrm{e}^{\mathrm{j}\omega})\mathbf{\Sigma}^{+}(\mathrm{e}^{\mathrm{j}\omega}) \sim \hat{\mathbf{G}}_{mi}(z), \tag{30}$$

$$\mathbf{G}_{ai}(\mathrm{e}^{\mathrm{j}\omega}) = \mathbf{U}^{\mathrm{H}}(\mathrm{e}^{\mathrm{j}\omega}) \sim \hat{\mathbf{G}}_{ai}(z). \tag{31}$$

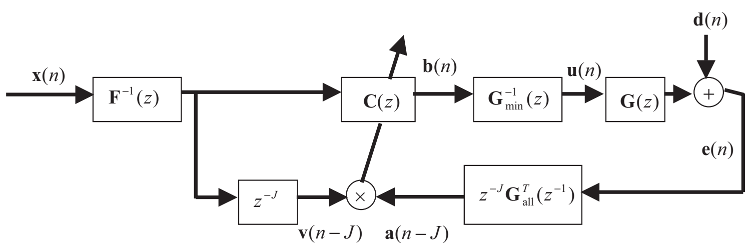

Fig. 4. Preconditioned multichannel LMS algorithm proposed in Ref. [10].

The symbol "$\sim$" in Eqs. (29)–(31) implies that the frequency responses approximate the Z transforms. Now that the above FIR filters have been calculated off-line, the adaptive system described in Fig. 4 is modified with the following substitution:

$$\mathbf{F}^{-1}(z) \rightarrow \hat{\mathbf{F}}_w(z), \quad (32)$$

$$\mathbf{G}_{min}^{-1}(z) \rightarrow \hat{\mathbf{G}}_{mi}(z), \quad (33)$$

$$z^{-J}\mathbf{G}_{all}^{\mathrm{T}}(z^{-1}) \rightarrow \hat{\mathbf{G}}_{ai}(z). \quad (34)$$

It is remarked that the subscripts "mi" and "ai" only symbolize the functional purpose (similar to Ref. [10]) of the filters, but no exact correspondence is implied. The resulting adaptive system is shown in the block diagram of Fig. 5, where the controller is updated according to the rule

$$\mathbf{C}_i(n+1) = \mathbf{C}_i(n) - \alpha\mathbf{a}(n)\mathbf{v}^{\mathrm{T}}(n-i), \quad (35)$$

with

$$\mathbf{a}(n) = \hat{\mathbf{G}}_{ai}(z)\mathbf{e}(n), \quad (36)$$

$$\mathbf{v}(n) = \hat{\mathbf{F}}_w(z)\mathbf{x}(n). \quad (37)$$

The adaptive system now implemented with the reference signals $\mathbf{x}(n)$ being processed by $\hat{\mathbf{F}}_w(z)$ to give $\mathbf{v}(n)$, which drives the controller $\mathbf{C}(z)$, and the output of $\mathbf{C}(z)$ is then multiplied by $\hat{\mathbf{G}}_{mi}(z)$ to generate the control signals $\mathbf{u}(n)$ for the plant. The vector of prewhitened signals $\mathbf{v}(n)$ is also required in the adaptation process, together with the filtered error signals, which are generated in this case by passing $\mathbf{e}(n)$ through the filter $\hat{\mathbf{G}}_{ai}(z)$. In order to implement the adaptive system with causal filters, however, J sample delays have been introduced in the procedure described in Section 2.2.

The adaptive system implemented with the block diagram shown in Fig. 5 avoids many of the convergence problems of the filtered error LMS algorithm. The reference signals are prewhitened and decorrelated by the filter $\hat{\mathbf{F}}_w(z)$. In addition, the transfer function from the output of the controller $\mathbf{b}(n)$ to the filtered error signals used to update this controller $\mathbf{a}(n)$ can be deduced by setting the disturbance to zero in Fig. 5. It can be easily verified that $\mathbf{a}(n)$ is equal to $\mathbf{b}(n)$, without any cross coupling, and the adaptation loop consists only of J sample delays.

$$\mathbf{a}(n) = \hat{\mathbf{G}}_{ai}(z)\mathbf{G}(z)\hat{\mathbf{G}}_{mi}(z)\mathbf{b}(n) \approx z^{-J}\mathbf{b}(n). \quad (38)$$

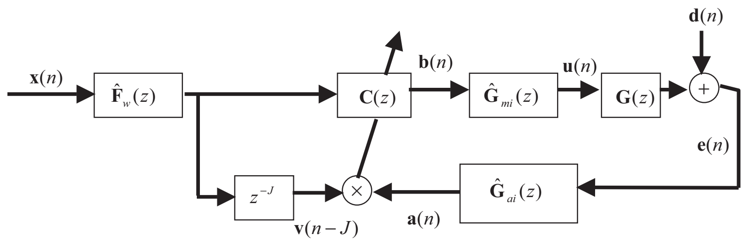

Fig. 5. Preconditioned multichannel LMS algorithm proposed in this paper.

Like the method presented in Ref. [10], the modified algorithm presented herein overcomes many of the causes of slow convergence in traditional filtered error and filtered reference LMS algorithms, via preconditioning the reference signals and the secondary plants. In comparison with the method in Ref. [10]; however, the present approach can be more effectively adapted to complicated high order plants, as generally encountered in acoustic problems because it requires no analytical form of factorizations during the design process.

3. Numerical simulation

A numerical investigation was carried out to justify the multichannel preconditioned LMS algorithms. Consider a CCS with two program signals (reference signals), two reproducing loudspeakers (secondary sources), and two receiving microphones (output sensors). In this case, $K=L=M=2$. The system arrangement is illustrated in Fig. 6. In audio applications, the audio program signals are generally colored and correlated. Two independent Gaussian white-noise signals n_1 and n_2 are used to generate the audio program signals available to the adaptive algorithm x_1 and x_2 via filters that give the reference signals a pink-noise spectrum (−3 dB/octave slope) and the mixing matrix of real numbers $\mathbf{M}$, which in this case was equal to

$$\mathbf{M} = \begin{bmatrix} 0.75 & 0.25 \\ 0.25 & 0.75 \end{bmatrix}. \tag{39}$$

In the arrangement for the LMS algorithm, the audio program signals are fed to a matrix of FIR filters $\mathbf{W}$, which produces u_1 and u_2 to drive the two secondary loudspeakers. The audio program signals are also delayed for 15 samples and used as the "desired" signals d_1 and d_2. Somewhat different from the active noise control application, the output signals y_1 and y_2 measured at the microphones at the listener's ears are compared with the corresponding desired signals to give the error signals e_1 and e_2. In the simulation, the sampling rate is selected to be 1 kHz. Each filter in $\mathbf{W}$ has 80 coefficients. The secondary loudspeakers, spaced 0.5 m apart, are assumed to operate under free field conditions, and are 1 m away from the output microphones which are symmetrically positioned 1 m apart.

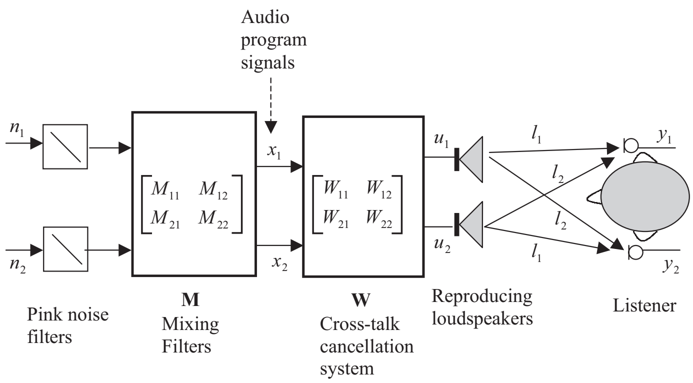

Fig. 6. Schematic diagram of the cross-talk cancellation system.

Because the secondary loudspeakers and the output microphones are symmetrically arranged, in free space, the continuous-time plant response can be written in this case as [16]

$$\mathbf{G}(j\omega) = \begin{bmatrix} \frac{A}{l_1}\mathrm{e}^{-\mathrm{j}kl_1} & \frac{A}{l_2}\mathrm{e}^{-\mathrm{j}kl_2} \\ \frac{A}{l_2}\mathrm{e}^{-\mathrm{j}kl_2} & \frac{A}{l_1}\mathrm{e}^{-\mathrm{j}kl_1} \end{bmatrix}, \quad (40)$$

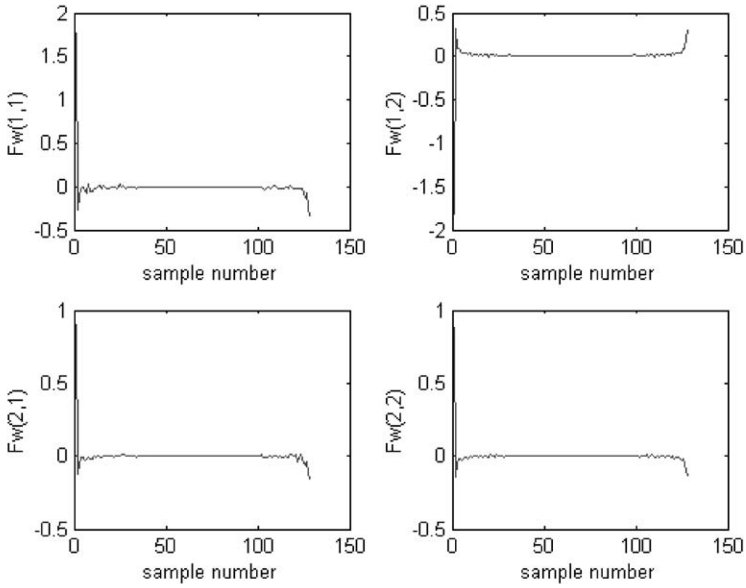

Fig. 7. Non-causal impulse responses of the prewhitening filters.

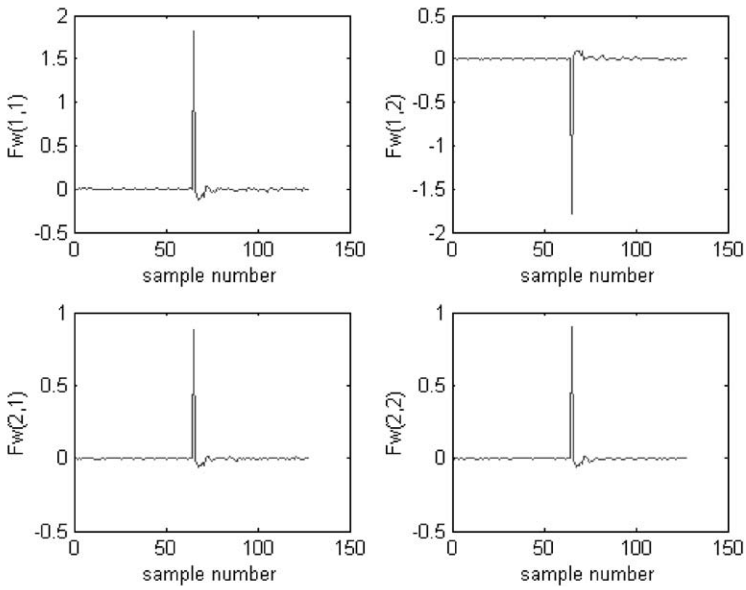

Fig. 8. Causal impulse responses of the prewhitening filters.

where A is an arbitrary amplitude constant, l_1 is the distance from the upper loudspeaker to the upper output microphone (1.03 m in this simulation), l_2 is the distance from the upper loudspeaker to the lower output microphone (1.25 m in this simulation), and k is the acoustic wave number, which is equal to ω/c_0, where ω is the angular frequency and c_0 is the speed of sound. If the signals are sampled at a rate of f_s, the normalized plant response matrix can be written in the z domain as

$$\mathbf{G}(z) = \begin{bmatrix} z^{-N_1} & \dfrac{l_1}{l_2} z^{-N_2} \\ \dfrac{l_1}{l_2} z^{-N_2} & z^{-N_1} \end{bmatrix}, \tag{41}$$

where N_1 is the nearest integer value of $l_1 f_s/c_0$, N_2 is the nearest integer value of $l_2 f_s/c_0$, and $l_1/l_2 < 1$ by definition. In this case, $\mathbf{G}(z)$ is a 2×2 square matrix.

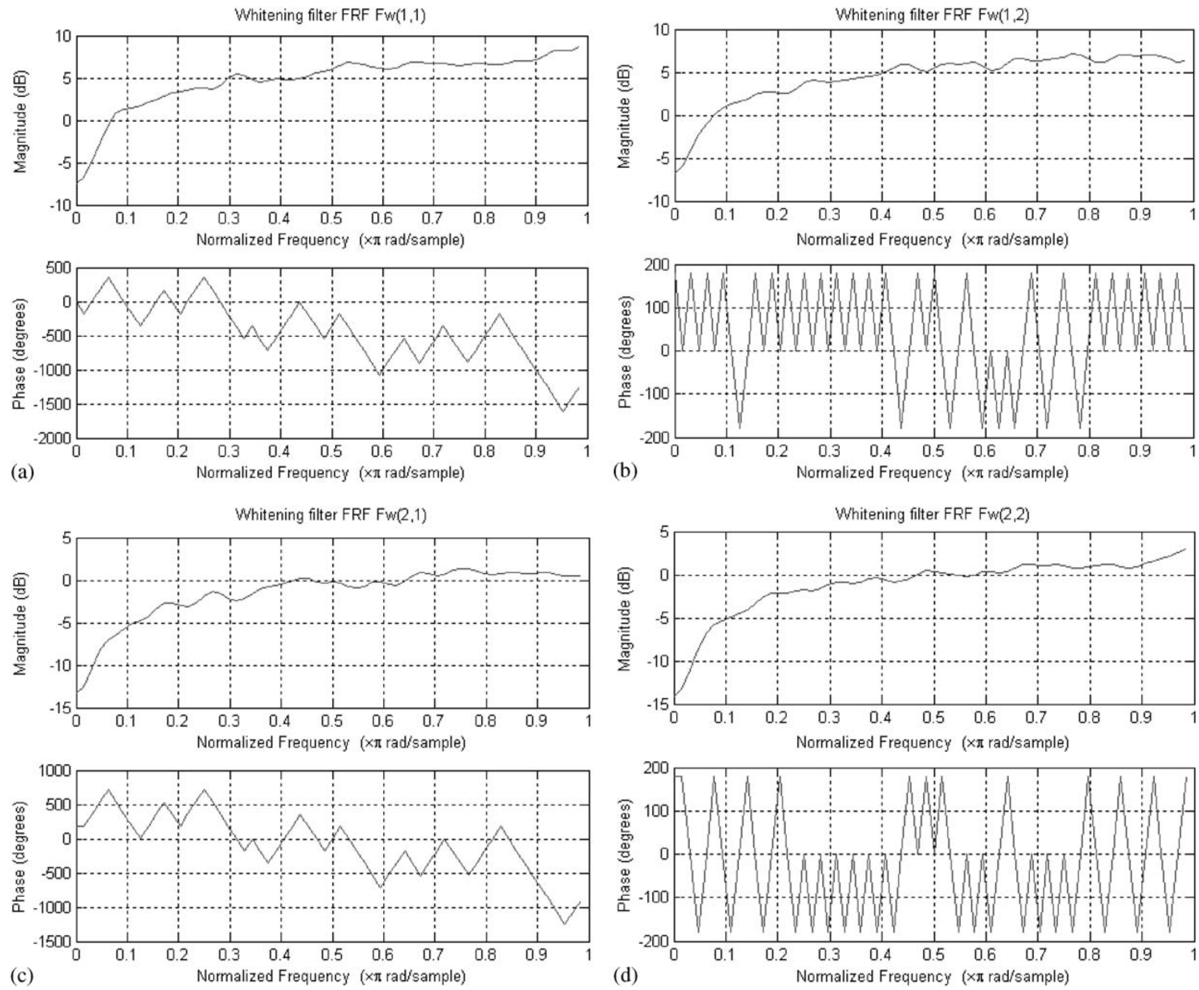

Fig. 9. The frequency response functions (FRF) of the prewhitening filters. (a) $F_w(1,1)$; (b) $F_w(1,2)$; (c) $F_w(2,1)$; (d) $F_w(2,2)$.

For this problem, the off-line design procedure presented in Sections 2.1 and 2.2 are conducted to obtain the prewhitening filters $\hat{\mathbf{F}}_w(z)$. In the procedure, 128-point FFT with 64 records of average was used for estimating the power spectral density matrix, $\mathbf{S}_{xx}(e^{j\omega})$, of the reference input signals. Fig. 7 shows the non-causal impulse response of the prewhitening filter $\hat{\mathbf{F}}_w(z)$, wrapped in the time domain due to the FFT. The rising tails of the four impulse responses can be clearly seen in the plot. Thus delay and truncation is applied to calculate causal FIR filters, as shown in Fig. 8. Because the power spectral density matrix is positive semi-definite symmetric [15], one-half of the FFT samples (64) is chosen as the delay number. Only 80 points in the impulse responses are retained to serve as the FIR filter coefficients, with the rest truncated. The associated frequency responses are also shown in Fig. 9. The high-pass nature of the prewhitening filers compensates for the low-pass pink-noise input. To further illustrate the prewhitening procedure, the power spectral densities of the reference signal 1 before and after prewhitening are shown in Fig. 10(a). In the procedure, 128-point FFT with 64 records of average was again used for estimating the

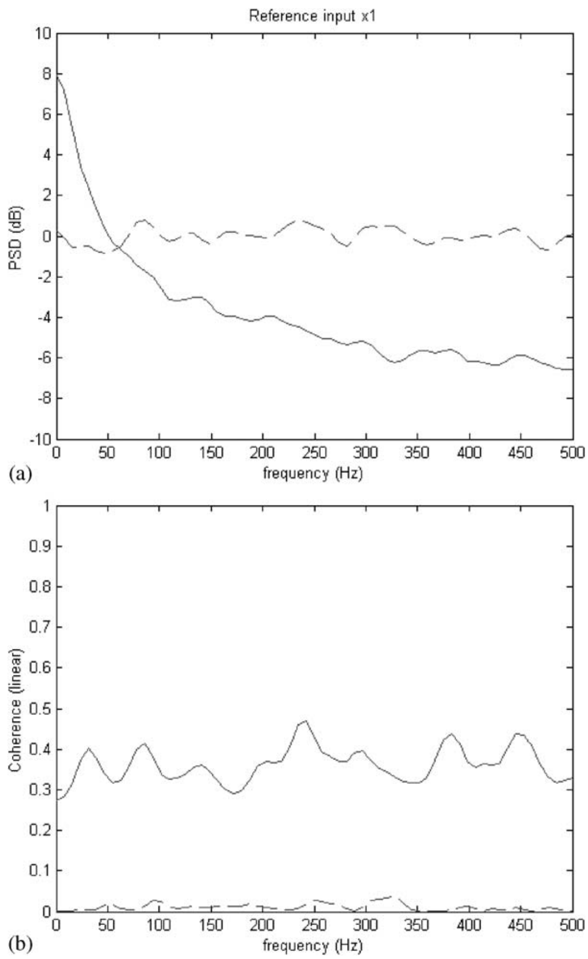

Fig. 10. Simulation results of the prewhitening procedure. (a) Power spectral density (PSD) of the reference signal 1. The result for the reference signal 2 is similar and is thus omitted. (b) Coherence between the reference signals 1 and 2.

power spectral density functions. The result indicates that the power spectral density of the signal becomes almost flat after prewhitening. The result for the reference 2 is quite similar and is thus omitted. The coherence between the two reference signals shown in Fig. 10(b) decreases from about 0.35 to nearly 0, which demonstrates the effectiveness of the decorrelation procedure.

In addition to the prewhitening filters, plant decoupling filters are also calculated according to the design procedure described in Section 2. For simplicity, only the impulse responses of the causal filters $\hat{\mathbf{G}}_{mi}(z)$ and $\hat{\mathbf{G}}_{ai}(z)$ are shown in Figs. 11 and 12, respectively. In order to obtain causal filters, a judicious choice has been made by introducing 20 sample delays in the design procedure. Furthermore, only 80 points in the impulse responses are retained to serve as the FIR filter coefficients, with the rest truncated. The resulting impulse responses of the plant, $\hat{\mathbf{G}}_{ai}(z)\mathbf{G}(z)\hat{\mathbf{G}}_{mi}(z)$, are calculated by using the decoupling filters. It can be seen in Fig. 13 that the plants have been effectively equalized and decoupled via the proposed procedure, with only pure delay terms in the diagonal entries of the impulse response matrix.

A simulation is conducted to compare the convergence properties of the various multichannel LMS algorithms: the LMS algorithm, the LMS algorithm with signal prewhitening only, the LMS algorithm with plant decoupling only, the LMS algorithm with both signal prewhitening and plant decoupling. Time histories of the reduction in the sum of squared error signal 1 for the simulation of the four multichannel LMS algorithms, with and without preconditioning, are shown in Fig. 14. In order to smooth the learning curves, 10 ensemble averages have been taken in plotting the results. The result for the error signal 2 is quite similar and is thus omitted. In all simulations, the convergence coefficient was set to half the lowest value that results in instability. Without preconditioning, the reduction achieved by using the ordinary LMS algorithm (denoted in the figure as "LMS") has only reached approximately 10 dB after 8000 samples of adaptation. If signal prewhitening is incorporated into the LMS algorithm (denoted in the figure as "LMS

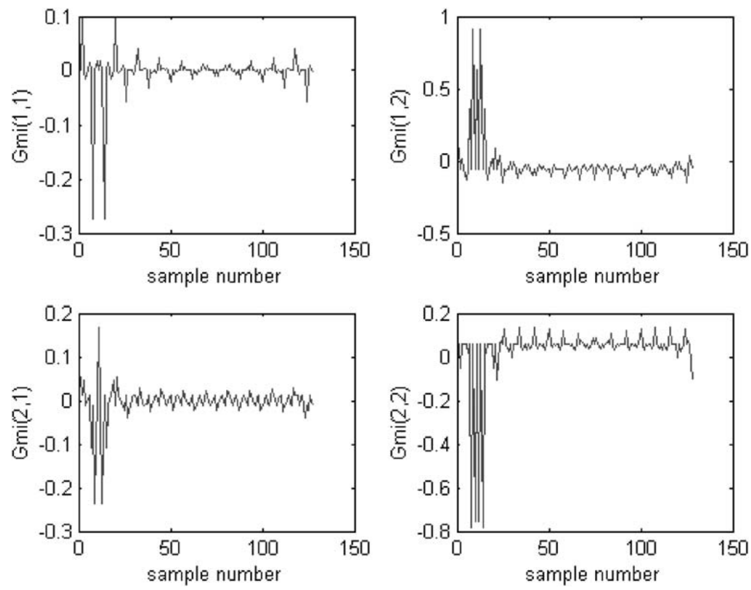

Fig. 11. Causal impulse responses of the filter $\hat{\mathbf{G}}_{mi}(z)$.

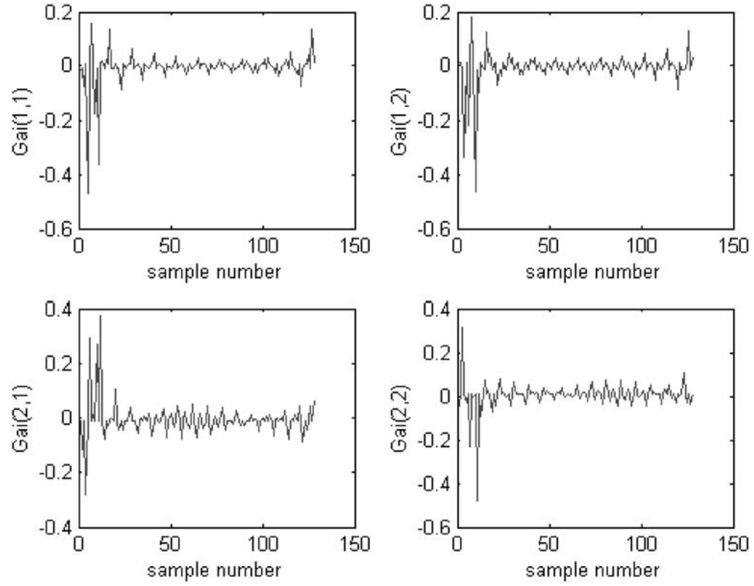

Fig. 12. Causal impulse responses of the filter $\hat{\mathbf{G}}_{ai}(z)$.

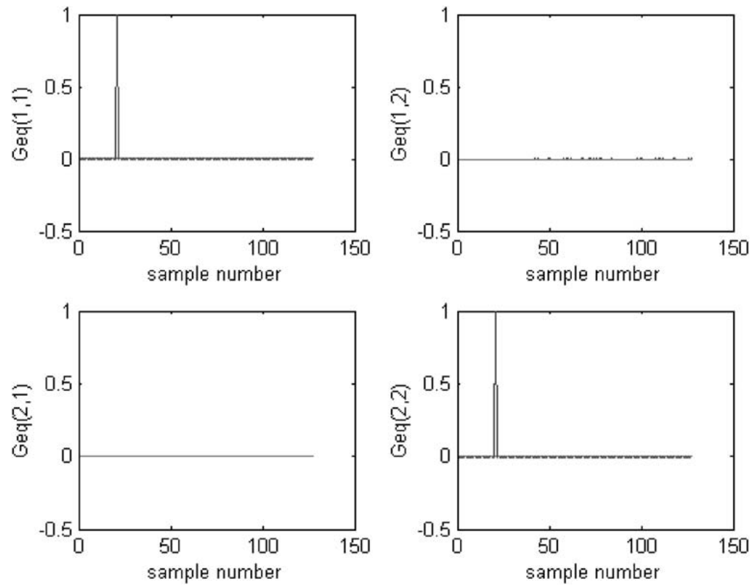

Fig. 13. Impulse responses of the decoupled plant matrix $\hat{\mathbf{G}}_{ai}(z)\mathbf{G}(z)\hat{\mathbf{G}}_{mi}(z)$, with 10 sample delays introduced.

with $\mathbf{F}_w$''), the reduction has reached approximately 18 dB after 8000 samples of adaptation. If plant decoupling is incorporated into the LMS algorithm (denoted in the figure as ''LMS with $\mathbf{G}_{dcp}$''), the reduction has reached approximately 20 dB after 8000 samples of adaptation. Finally, if both signal prewhitening and plant decoupling are incorporated into the LMS algorithm

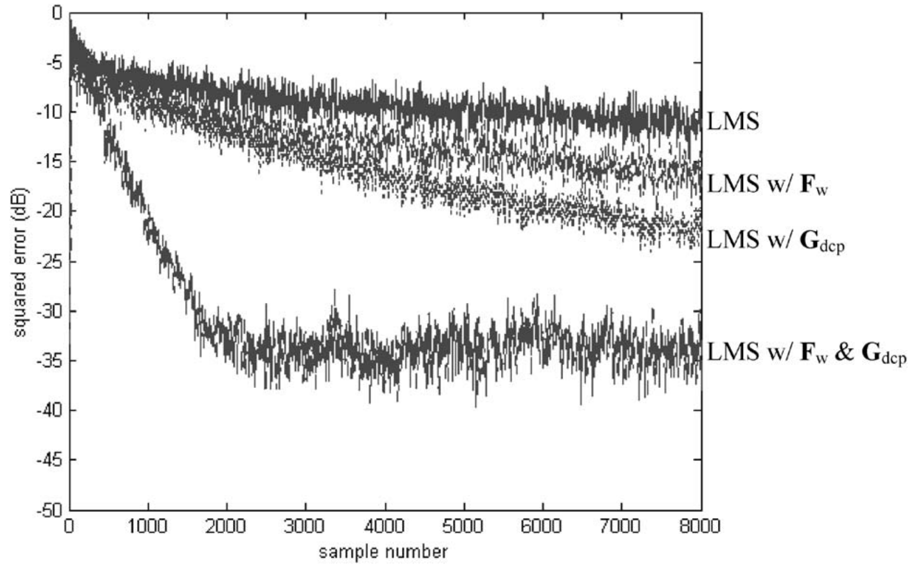

Fig. 14. Time histories of the reduction in the sum of squared error signal 1 for the simulation of four multichannel LMS algorithms, with and without preconditioning. The result for the error signal 2 is similar and is thus omitted. "LMS" denotes the ordinary LMS algorithm without preconditioning. "LMS with $\mathbf{F}_w$" denotes the LMS algorithm with signal prewhitening. "LMS with $\mathbf{G}_{dcp}$" denotes the LMS algorithm with plant decoupling. "LMS with $\mathbf{F}_w$ and $\mathbf{G}_{dcp}$" denotes the LMS algorithm with both signal prewhitening and plant decoupling.

(denoted in the figure as "LMS with $\mathbf{F}_w$ and $\mathbf{G}_{dcp}$"), the fastest convergence has occurred for which 35 dB reduction has been achieved in about 3000 samples of adaptation.

4. Conclusion

A preconditioning technique has been developed in this paper for the multichannel LMS algorithm to improve the convergence rate. Signal prewhitening and system decoupling are two key elements of the proposed technique. Preconditioning filters are first formulated in the frequency domain by using EVD of the signal power spectral density matrix and SVD of the plant frequency response matrix. The filters are then converted to the time domain with causality taken into account. The preconditioning filters have been incorporated into a multichannel LMS algorithm, where the reference signals are prewhitened and the plants are decoupled prior to the adaptation process. As compared to a similar method in Ref. [10], the present technique has the advantage that it does not rely on any difficult model-based computation of matrix-valued spectral factorization and minimum-phase/all-pass decomposition, which is a desirable feature for practical applications. Simulations for a two-channel/one listener CCS demonstrated that the proposed preconditioning technique results in faster convergence rate of LMS algorithms than the non-conditioned or partially conditioned algorithms.

As a limitation of the proposed method, a linear phase shift will generally be introduced as a result of the inherently frequency-domain formulation. How much truncation and delay should be employed for a particular problem to obtain causal filters remains largely ad hoc and empirical. For the audio signal processing application in this paper, pure delay will not result in waveform distortion. In other applications such as active control, however, system delay may become a critical issue [17]. It is thus worth exploring in the future research the difference between the results calculated using the method proposed in this paper and the method using model-based spectral factorization, and also the effects of various preconditioning approaches on the multichannel adaptive algorithms.

Acknowledgements

This project was sponsored by the National Science Council (NSC) in Taiwan under the project number NSC 89-2212-E-009-007. This study was completed during the visit of the first author in April 2002 in the Institute of Sound and Vibration Research (ISVR), University of Southampton, UK.

References

[1] S.J. Elliott, P.A. Nelson, Active noise control, IEEE Signal Processing Magazine 10 (1993) 12–35.
[2] S.J. Elliott, Signal Processing for Active Control, Academic Press, New York, 2001.
[3] B. Widrow, E. Walach, Adaptive Inverse Control, Prentice-Hall, Upper Saddle River, NJ, 1996.
[4] J. Minkoff, The operation of multichannel feedforward adaptive systems, IEEE Transactions on Signal Processing 45 (1997) 2993–3005.
[5] P.A. Nelson, H. Hamada, S.J. Elliott, Adaptive inverse filters for stereophonic sound reproduction, IEEE Transactions on Signal Processing 40 (7) (1992) 1621–1632.
[6] P.A. Nelson, F. Orduna-Bustamante, Multi-channel signal processing techniques in the reproduction of sound, Journal of Audio Engineering Society 44 (1996) 973–989.
[7] J. Cook, S.J. Elliott, Connection between multichannel prediction error filter and spectral factorisation, Electronics Letters 35 (15) (1999) 1218–1220.
[8] S.C. Douglas, A. Cichocki, S.I. Amari, Self-whitening algorithms for adaptive equalisation and deconvolution, IEEE Transactions on Signal Processing 47 (4) (1999) 1161–1165.
[9] I. Proudler, I. Skidmore, J. McWhirter, Increasing the performance of the LMS algorithm using and adaptive preconditioner. Proceedings of the Eighth European Signal Processing Conference (Ensipco), N. Xp-000979686, pp. 1385–1388.
[10] S.J. Elliott, Optimal controllers and adaptive controllers for mutichannel feedforward control of stochastic disturbances, IEEE Transactions on Signal Processing 48 (4) (2000) 1053–1060.
[11] T. Kailath, A.H. Sayed, B. Hassibi, Linear Estimation, Prentice-Hall, Upper Saddle River, NJ, 1977.
[12] B. Widrow, S.D. Stearns, Adaptive Signal Processing, Prentice-Hall, Englewood Cliffs, NJ, 1985.
[13] S. Hykin (Ed.), Blind Deconvolution, Prentice-Hall, Englewood Cliffs, NJ, 1994.
[14] B. Nobel, J.W. Daniel, Applied Linear Algebra,, Prentice-Hall, Upper Saddle River, NJ, 2000.
[15] J.A. Cadzow, Foundations of Digital Signal Processing and Data Analysis, MacMillan, New York, 1987.
[16] L.E. Kinsler, A.R. Frey, A.B. Coppens, J.V. Sanders, Fundamental of Acoustics, Wiley, New York, 1982.
[17] M.R. Bai, Y. Lin, J.W. Lai, Reduction of electronic delay in active noise control systems—a multirate signal processing approach, Journal of Acoustic Society in America 111 (2) (2002) 916–924.